Title: Transdifferentiation of fibroblasts into muscle cells to constitute cultured meat with tunable intramuscular fat deposition

Tongtong Ma [1, 2, #], Ruimin Ren [1, 2, #], Ruipeng Yang [1], Zheng Xinyi [1, 2], Yang Hu [3], Guiyu Zhu [1], Heng Wang [1, 2, *]

[1] College of Animal Science and Technology, Shandong Agricultural University, Taian, China

[2] College of Animal Science and Technology, Huazhong Agricultural University, Wuhan, China

[3] College of Food Science and Technology, Huazhong Agricultural University, Wuhan, China

# These authors contributed equally to this work.

* Corresponding author: wangheng@mail.hzau.edu.cn

Abstract

Current studies on cultured meat mainly focused on the muscle tissue reconstruction in vitro, but lack the formation of intramuscular fat which is a crucial factor in determining taste, texture and nutritional contents. Therefore, incorporating fat into cultured meat is of superior value. In this study, we employed the myogenic/lipogenic transdifferentiation of chicken fibroblasts in 3D to produce muscle mass and deposit fat into the same cells without the co-culture or mixture of different cells or fat substances. The immortalized chicken embryonic fibroblasts were implanted into the hydrogel scaffold and the cell proliferation and myogenic transdifferentiation were conducted in 3D to produce the whole-cut meat mimics. Compare to 2D, cells grown in 3D matrix showed elevated myogenesis and collagen production. We further induced fat deposition in the transdifferentiated muscle cells and the triglyceride content could be manipulated to match and exceed the levels of chicken meat. The gene expression analysis indicated that both lineage-specific and multi-functional signalings could contribute to the generation of muscle/fat matrix. Overall, we were able to precisely modulate muscle, fat, and collagen content according to balanced or specialized meat preferences. These findings provide new avenues for customized cultured meat production with desired intramuscular fat contents that can be tailored to meet the diverse demands of consumers.

Introduction

Cultured meat is an innovative and emerging technique that produces meat directly from cell cultures, potentially providing a high-quality, safe, and stable source of animal protein (Chriki and Hocquette, 2020). In comparison to traditional livestock and poultry farming, cultured meat generates fewer greenhouse gases, utilizes less arable land, and causes less animal harm (Mattick et al., 2015). Proper selection of seed cells is one of the keys to the success of cultured meat production. The starting cells must be easily obtainable and be able to proliferate numerous times to enable mass production. While the stem cells like muscle stem cells and pluripotent stem cells have frequently been utilized as the cellular source for cultured meat, these stem cells are rare in the animal body and difficult to obtain and amplify on a large scale. In contrast, the somatic cells, which constitute the body, could be efficiently converted into muscle cells under certain conditions. The fibroblast is one of the most abundant and widely-distributed cell types present in the body and could be easily collected via minimally invasive biopsy procedure without sacrifice the farm animals. The fibroblasts can replicate indefinitely in vitro and are amenable for myogenesis, adipogenesis and chondrogenesis (French et al., 2004; Yin et al., 2010), which produce muscle, fat and extracellular matrix (ECM) proteins that constitute the meat and the associated texture and flavor. Recently, the fibroblast cells from farm animals have been utilized as the source cells for cultured meat production, with or without myogenesis (Jeong et al., 2022; Pasitka et al., 2023), demonstrating the feasibility of somatic cell-derived seed cells as a sustainable and ethical option for cultured meat production.

We have previously developed a protocol for the controlled transdifferentiation of chicken fibroblasts into myoblasts, which subsequently form multinucleated myotubes and express mature muscle proteins (Ren et al., 2022). Moreover, chicken fibroblasts could also be efficiently converted into fat-depositing lipocytes by treating them with chicken serum medium or other substances such as fatty acids (Hausman, 2012; Kim et al., 2020; Lee et al., 2021). Therefore, the induced myogenic and adipogenic competency, along with the native fibrogenic collagen-producing ability of chicken fibroblasts, can enable us to simultaneously synthesize muscle, fat and collagen during the cultured meat production. Nevertheless, further techno-functional research is necessary to precisely control the composition of the end product of fibroblast-derived cultured meat in order to achieve a more balanced and personalized nutritional profile and meet the specific consumer preferences.

In this study, the chicken fibroblast cells were implanted into the hydrogel scaffold to analyze the 3D cellular dynamics involving cell proliferation and myogenic/adipogenic transdifferentiation. We also optimized the low-serum culture conditions of chicken fibroblasts to reduce the cost of mass production. The myogenic transdifferentiated cells were confirmed to be skeletal muscle lineage but not myofibroblasts. Importantly, the cells were subjected to myogenesis and adipogenesis sequentially in 3D hydrogel matrix to resemble the whole-cut meat with the controllable intramuscular fat and collagen content. By using transdifferentiation strategies, the depositing ratio of fat into the cultured meat could be manually and precisely adjusted, allowing the nutrients to be naturally synthesized from the organized muscle structure. This demonstrates the potential for manipulating cultured meat to meet consumer preferences for specific fat content and texture.

Results

Chicken fibroblasts proliferate stably in low-serum conditions

The chicken fibroblast cells were chosen as the source cell for cultured meat production because they can propagate indefinitely and undergo myogenesis whenever the induction is provided. We have previously constructed an inducible myogenic transdifferentiation system in chicken fibroblasts with the stable integration of Tet-On-MyoD cassette (Ren et al., 2022). The MyoD is the key myogenic transcription factor and the chicken fibroblasts could be converted into striated and elongated myotubes (myofibers) upon forced expression of MyoD (Ren et al., 2022; Weintraub et al., 1989). The Tet-On-MyoD cassette enables the inducible and reversible activation of chicken MyoD factor, and in the current fibroblast cells, the myogenic transdifferentiation is only switched on by adding doxycycline (DOX). Without the DOX treatment, the control chicken fibroblast cells (Tet-On-MyoD) do not differ from the wild-type cells in terms of morphology, proliferation rate and gene expression (Figure S1A). Hence, as a proof-of-concept experiment, we utilized this inducible myogenic fibroblast cell line to develop protocols for cultured chicken meat production.

To achieve sustainable and cost-effective cell production, it is essential to minimize the serum usage in the culture medium. Therefore, we implemented a progressive serum reduction approach to acclimate the cells in the prospect of obtaining a stable cell source that can be propagated in low serum concentrations. In the initial experiment, we used 12% fetal bovine serum (FBS) in 1640 basal medium, which served as the control group.

The results showed that the cells were able to proliferate normally at 6%, 3% and 1.5% serum concentrations, but at decreasing rates as shown by the EdU assay (Figure 1A and 1B). We also tested the chicken serum as an alternative to bovine serum, in order to avoid cross-species contamination of animal derivatives. The results showed that chicken fibroblasts could proliferate stably in the 1% chicken serum (Figure 1A and 1B) and the cell populations multiply 3 times in 3 days as demonstrated by the CCK-8 assay (Figure 1C). Thus, we conclude that the low-serum medium can effectively support the stable propagation of chicken fibroblasts.

3D culture of chicken fibroblasts in GelMA hydrogels

The behavior of cells grown on the top of 2D flat surface may differ from that of cells in 3D space. To simulate the 3D natural growth environment of cells *in vivo*, we utilized the Gelatin Methacrylate (GelMA)-based hydrogels as scaffolds for chicken fibroblasts. GelMA hydrogel can form a stable and porous structure for cell implantation and is commonly used in tissue engineering and food processing because of its great biocompatibility and mechanical tenability (Pepelanova et al., 2018). We created hydrogels with varying concentrations at 3%, 5%, 7%, 9%, and then observed their surface characteristics when immersed in culture medium using an emission scanning electron microscope. The porosity was measured to be 83.27%, 65.01%, 62.47% and 57.96%, respectively. Thus, the higher the mass concentration of hydrogels, the tighter the 3D mesh structure formed and the smaller the porosity (Figure 2A). The pore diameters in the scaffolds were determined to range from $3\mu m^2$ to $100\mu m^2$, showing the biggest pore size in 3% hydrogel and smallest in 9% hydrogel (Figure 2B). Therefore, the porosity and pore size of the scaffold could be adjusted to achieve optimal physical strength and nutrients delivery that suited for long-term cell culturation.

To determine the most ideal gel concentration and pore size suited for chicken fibroblast attachment and growth, we conducted an experiment where we implanted the same number of cells into gels with varied pore sizes and examined the cellular dynamics over a 9-day period (Figure S2). The cells adhered to the gels immediately and started to exhibit typical extended and irregular fibroblast cell morphology after 1 day, indicating the hydrogel's good biological compatibility with chicken fibroblast cells. However, the 3% hydrogel collapsed in the medium 2 days after cell implantation and thus did not support the long-term cell growth. We continued to monitor the 3D cell proliferation and found that the cells successfully propagated in 5%, 7%, 9% hydrogels

126 for the entire duration of the experiment. Among the tested hydrogels, the 5%
127 concentration was found to be the best option for cell attachment and growth as shown
128 by the densest cellular structure formed, and thus be utilized for the subsequent analysis.
129
130 Due to the challenges of observing and distinguishing the cells and pores within the
131 hydrogel scaffold using the brightfield of ordinary light microscopy, we then used the
132 PKH26 fluorescent cellular dye to accurately observe the cellular morphology and
133 quantity the cell numbers. The cells were firstly labelled with PKH26 in 2D culture
134 (Figure S3A) and then transferred into the gel matrix. Upon implantation, the cells
135 appeared mostly round on the first day, but gradually extended and expanded in number
136 within the hydrogel scaffold. By the 5th day, most of the cells were elongated with
137 irregular shape and short tentacles and packed tightly, and by the 9th day they had
138 grown densely and formed fibrous bundles (Figure 2C). We also examined the
139 proliferation dynamics of the cells in 3D scaffold via the EdU assay. The proliferation
140 efficiency of chicken fibroblast cells gradually increased overtime in 3D culture and
141 reached replication levels even higher than those in 2D culture (Figure 2D and 2E). This
142 result indicates that 3D culture conditions provide a more favorable environment for
143 cell growth. Moreover, when the 3D cultured cells were detached from the gel by
144 collagenase dissociation (Figure S3B) and seeded back in 2D monolayer culture plates,
145 the cells again exhibited similar morphology but slightly increased proliferation
146 capacity compared to the original fibroblasts in 2D conditions (Figure S3C and S3D).
147 Thus, the chicken fibroblast cells cultured in 3D maintain their normal physiological
148 characteristics and we continue to stimulate the cellular myogenesis and lipogenesis to
149 prepare them for cultured meat production.
150
151 **Transdifferentiation of chicken fibroblasts into muscle cells in 3D**
152 Despite the complexity in the composition of fresh meat and processed products,
153 muscle cells are the major and indispensable component of meat foods. The muscle cell
154 derived myotubes (myofibers) provide a rich source of proteins and nutrients and
155 constitute the meat texture. To this end, we aimed to transform the chicken fibroblast
156 into muscle cells through the established MyoD overexpression protocol (Ren et al.,
157 2022). We first tested and optimized the myogenic transdifferentiation parameters in
158 2D culture through the DOX induced MyoD expression. We observed elongated
159 multinucleated myotubes and abundant expression of myosin heavy chain (MHC) after
160 3 days of myogenic induction (Figure S4A). The “serum deprivation” protocol was the

classical strategy to stimulate terminal myogenic differentiation in myoblasts of various species including chicken (Nakashima et al., 2005). Thus, we examined the myogenic transdifferentiation efficiency (myotube fusion index) in the chicken fibroblast cells overexpressing MyoD in combination with reduced concentrations of bovine or horse serums. However, we found that reducing serum concentrations did not increase the myotube formation but instead caused massive cell death instead (Figure S4B). Therefore, it seems that the "serum deprivation" could not further improve the myogenic transdifferentiation in chicken fibroblast cells and a simple MyoD overexpression strategy is sufficient for efficient production of mature muscle cells.

After demonstrating the feasibility of induced transdifferentiation of chicken fibroblasts into muscle cells in 2D culture, we continued myogenic transdifferentiation in 3D to simulate the construction of concrete whole-cut meat. The cells were inoculated into a hydrogel scaffold and allowed to proliferate for 7 days before inducing transdifferentiation with MyoD overexpression (Figure 3A). We used whole-amount MHC immunofluorescence staining to examine the myotube formation directly inside the gel. We identified abundant multinucleate MHC^{+} myotubes at multiple focal planes within the gel (Figure 3B, Supplementary Video1), indicating successful myogenic transdifferentiation of 3D cultured chicken fibroblasts. In contrast, there were no MHC signal or autofluorescence detected in the 3D cultured chicken fibroblasts (Figure S4C) and hydrogel without cells (Figure S4D). With the assistance of confocal Z-stack analysis, the stacked images showed densely packed MHC+ myotubes from a piece of cellular hydrogel complex at a depth of 68 μm (Figure 3D). The separate XY axis views of the orthogonal projections at different depths (Figure 3D) and a multi-angle video (Supplementary Video 2) also showed the myotubes aligned in three dimensions. Therefore, we successfully transformed the chicken fibroblast cells into muscle cells in 3D environment.

Compared to 2D, the transdifferentiated myotubes induced in 3D were more organized and densely packed, resembling the native myofiber distribution *in vivo* (Figure 3B). And the myotube formation efficiency (fusion index) in 3D reached 30.49%, which was significantly higher than that of the 2D under the same transdifferentiation conditions (Figure 3C). We also evaluated the expression of several myogenic markers by RT-qPCR (Figure 3F). MyoG (Myogenin) is a transcription factor regulating terminal skeletal muscle differentiation and could be induced by MyoD (Cao et al., 2006).

MYH6 (Myosin Heavy Chain 6) is the major protein comprising the muscle thick filament, and functions in muscle contraction (van Rooij et al., 2009; Warkman et al., 2012). MCK (Muscle Creatine Kinase) is an enzyme that primarily active in mature skeletal and heart muscle (Vincent et al., 1993). However, all myogenic factors, including MyoG, MYH6, and MCK, significantly increased upon transdifferentiation in both 2D and 3D. In addition, the transdifferentiated cells exhibited much higher expression of MyoG and MCK in 3D conditions compared to that in 2D, indicating more robust myogenic differentiation and maturation of cells in the 3D microenvironment. We speculate that the porous structure of the hydrogel matrix may support the cells to grow in all directions, similar to the environment in which the myofibers form in vivo.

Macroscopically, the muscle filaments and the dense cellular network structures formed by myogenic transdifferentiation could make the hydrogel matrix more compact and solid (Figure 3G). Thus, compared to the empty transparent scaffolds without cells, the hydrogels cultivated with muscle cells are more visually like whole-cut meat thus resemble to the fresh animal meat.

Myogenic transdifferentiation of fibroblast does not produce myofibroblasts

Fibroblasts can be induced to differentiate into myofibroblast upon injury, leading to tissue fibrosis. Similar to the skeletal muscle cells, the myofibroblast are also contractile and express the myogenic factor MyoD as well as certain types of sarcomeric myosin heavy chains (MHC) (Hecker et al., 2011). To confirm that the myogenic transdifferentiated cells were indeed skeletal muscle cells but not the myofibroblasts, we utilized a panel of cell lineage-specific markers to delineate the cell conversion progress and determine the cellular identity of fibroblasts, myoblasts and myofibroblasts, respectively. The immunofluorescence staining of 3D cultured cells showed that the muscle-specific intermediate filament Desmin (Paulin and Li, 2004) was expressed only in the MyoD transdifferentiated cells, but not in the original fibroblasts or the embryonic skin derived myofibroblasts (Figure 4A). In contrast, the classical myofibroblast marker alpha-smooth muscle actin (α-SMA) (Hinz et al., 2007; Takase et al., 1988) was expressed only in myofibroblasts, but not in the fibroblast or the transdifferentiated cells (Figure 4B). The fibroblast intermediate filament Vimentin (Tarbit et al., 2019) was abundantly expressed in the fibroblasts and myofibroblasts but greatly reduced in the myogenic transdifferentiated cells (Figure 4C). The 2D and 3D

231 cultured cells showed consistent pattern of marker protein expression, indicating that
232 the different culture models and conditions do not affect the cell identity conversion
233 (Figure S5A and S5B). These results confirmed that the MyoD indeed transdifferentiate
234 the cells toward the skeletal muscle lineage but not the myofibroblast. Furthermore, the
235 RT-qPCR showed that, after myogenic induction in 3D, the skeletal muscle specific
236 genes Desmin and Six1 (Relaix et al., 2013) were significantly elevated (Figure 4D)
237 whereas the fibroblast gene Thy-1 was significantly reduced (Figure 4E). The
238 transforming growth factor β (TGFβ) signaling is the most potent known inducer of
239 myofibroblast differentiation (Vaughan et al., 2000). We found the expression of core
240 TGFβ signaling components, TGFβ-1, TGFβ-3 and Smad3, remain unchanged during
241 the transdifferentiation process (Figure 4F), indicating that the classical myofibroblast
242 lineage was not induced. Together, these data confirm that the myogenic
243 transdifferentiation of fibroblast does not produce myofibroblasts.
244
245 **Stimulate the fat deposition in chicken fibroblasts in 3D**
246 The intramuscular fat is a crucial component of meat that can determine its quality
247 attributes, such as taste and flavor. The chicken fibroblasts have been reported to be
248 amenable for lipogenesis through various stimulus, including chicken serum, insulin,
249 fatty acids and retinoic acids (Kim et al., 2021; Kim et al., 2020; Lee et al., 2021). We
250 first attempted different lipogenic stimulations on 2D cultured cells and stained them
251 for Oil Red O to visualize and quantify fat deposition in the fibroblasts. Only very few
252 scattered Oil Red O signals were found in the treatments consisting of only serums
253 (12.5% FBS, 1% chicken serum or 2% chicken serum), indicating no lipogenesis during
254 normal proliferation conditions. However, when we added insulin and fatty acids
255 (oleic/linoleic acid) to the medium, lipid droplets in the cells dramatically increased as
256 detected by the Oil Red O staining. After extensive optimization of the concentrations
257 of supplements in the medium, we identified that the 8μg/ml fatty acids plus 60μg/ml
258 insulin (abbreviated as FI, F: fatty acids, I: insulin) can induce lipogenesis most
259 efficiently in 2D chicken fibroblasts (Figure S6A and S6B).
260
261 Next, the same lipogenesis induction strategy was applied to the 3D cultured cells. We
262 found extensive Oil Red O signal inside the hydrogel matrix at different focal planes
263 and the lipid droplets were clearly visible as beaded strings under magnification (Figure
264 5A and 5B, Supplementary Video3). The RT-qPCR analysis illustrated the expression
265 of genes involved in lipogenesis and triglyceride synthesis were significantly higher in

266 the cells with lipogenic stimulation compare to the control (Figure 5C). Notably, the
267 genes encoding for PPARγ (peroxisome proliferator-activated receptor gamma), Gpd1
268 (glycerol-3-phosphate dehydrogenase) and FABP4 (fatty acid binding protein 4) all
269 showed higher expression in 3D than that in 2D. Interestingly, the expression of Znf423
270 (zinc finger protein 423), which is a PPARγ transcriptional activator (Addison et al.,
271 2014; Longo et al., 2018), only increased upon lipogenic induction in 3D but not in 2D
272 conditions. It seems that the cells grown in 3D hydrogel showed enhanced lipogenesis
273 compare to the flat surface cultured cells, similar to the myogenic transdifferentiation
274 process in 3D. In addition to the lipogenic induction with fatty acids and insulin (FI),
275 we also validated the use of chicken serum in promoting lipid accumulation as previous
276 reported (Kim et al., 2021). Our results showed that the chicken serum alone could also
277 stimulate fat accumulation effectively (Figure S6C and S6D). We further measured the
278 triglyceride content and found that the lipogenic induction increased the triglyceride
279 significantly in the cell matrix (Figure 5D). In conclusion, the 3D cultured chicken
280 fibroblast can efficiently deposit lipid by different stimulus.
281
282 **Controlled fat deposition in the transdifferentiated muscle cells in 3D hydrogel**
283 The above presented data shows that chicken fibroblast cells have a superior capacity
284 for transforming into muscle and depositing fat when cultured in a 3D hydrogel matrix.
285 Next, we tried to combine the myogenic and lipogenic stimuli together to modulate the
286 fat deposition in the cultured meat to simulate the various intramuscular fat contents in
287 the conventionally raised meat. Rather than converting fibroblasts into muscle cells and
288 fat cells separately and mixing them later, we adopted a new strategy that can induce
289 de novo lipid deposition in the muscle by first inducing myogenic transdifferentiation
290 and then followed by lipid induction in the same cells (Figure 6A and S7A). In 2D
291 conditions, plenty of MHC^+ myotubes and Oil Red O-stained lipids were found to
292 intermingle after the myogenic/lipogenic treatment (Figure S7B) and some of the red
293 marked lipid droplets were located inside the myotubes, indicating that the transformed
294 muscle cells indeed deposit fat autonomously (Figure S7C). Next, we applied the
295 similar treatment to the cells cultured in 3D hydrogel and also identified Oil Red O-
296 labelled lipid droplets mixed with the densely packed MHC^+ myotubes (Figure 6B and
297 6C). These findings suggest that the use of myogenic/lipogenic treatments can induce
298 the formation of muscle cells that are capable of depositing fat in both 2D and 3D. We
299 further examined the expression levels of both myogenic and lipogenic factors in the
300 3D cultured cells by RT-qPCR. Compare to the control 3D cells without

301 myogenic/lipogenic stimulations, the induced cells showed significantly higher
302 expression of genes involved in both myogenesis and lipogenesis (Figure 6D).
303 Interestingly, the extent of gene upregulation upon the combined myogenic/adipogenic
304 stimulations was comparable to that of myogenic or adipogenic induction alone. This
305 finding suggests that sequential myogenic transdifferentiation and lipid deposition do
306 not interfere with each other when conducted in the same cells.
307
308 The intramuscular fat is an integral component of both the traditional animal meat and
309 the cultured meat, and it directly influences the meat flavor and texture (Frank et al.,
310 2016). Hence, we compared the triglyceride levels in the 3D hydrogel cells with
311 different types of lipogenic stimuli with the chicken breast and leg meat. The results
312 showed that the lipogenic stimulation in the 3D hydrogel cells increased the triglyceride
313 content in the cultured meat to the levels comparable or even higher than real chicken
314 meat (Figure 6E). In contrast, the control cells without any induction or with only
315 myogenic stimulation do not show apparent triglyceride accumulation (Figure 6E).
316 Therefore, the fat content in the cultured meat could be synthesized by a controlled
317 manner and then we tried to purposely manipulate the triglyceride contents in the meat
318 matrix by adjusting the potency of adipogenic stimulation. By fine-tuning the
319 concentrations of insulin and fatty acids during lipogenic induction, the triglyceride
320 contents in the final product of cultured meat can precisely reach any customized levels
321 across the range from 1.5mg/g to 7mg/g (Figure 6E), which overlap and surpass the
322 levels in the fresh chicken breast and leg meat. As a result, this strategy greatly expands
323 the diversity and category of cultured meat products, allowing for precise control over
324 intramuscular fat contents to meet consumer preferences. Therefore, guided and graded
325 fat deposition in cultured meat allows for the creation of various meat products with
326 controlled intramuscular fat contents.
327
328 **The collagen content and ECM components of cultured meat**
329 Fibroblasts are an essential source of extracellular matrix (ECM) including the collagen,
330 which providing elasticity to the tissue in the body and enriching the texture of the
331 cultured meat (Ben-Arye and Levenberg, 2019). In theory, the fibroblast should produce
332 abundant ECM to produce a more realistic meat product. We then examined the
333 collagen content in the cultured meat and found that the total collagen protein gradually
334 increased and reached the plateau at 1.59 μg/mg in the final product (Figure 7A). This
335 is mainly due to the increased cell numbers and the accumulation of secreted collagen

336 in the hydrogel matrix. Nevertheless, the RT-qPCR showed that the genes encoding the
337 major components of ECM exhibited various expression patterns with the extension of
338 culture time. The expression of COL1A1 (Collagen, type I, alpha 1) and COL1A2
339 (Collagen, type I, alpha 2) gradually decreased, whereas the fibronectin increased
340 during the time course of meat synthesis. The expression of elastin and laminin genes
341 remain stable throughout the whole course of experiment (Figure 7B). Overall, the
342 synthesis and accumulation of different types and amounts of ECM components during
343 the myogenic/lipogenic stimulations can improve the texture of the cultured meat
344 prepared from fibroblast cells.

345 **The characterization of molecular changes during myogenic transdifferentiation**
346 **and fat deposition in cultured meat**

347 To provide insights into the functional shifts during the transdifferentiation from
348 fibroblasts toward muscle, fat, or muscle/fat cells in 3D culture, we further analyzed
349 the transcriptomes from the different populations of cells including the "original
350 fibroblasts" (3D_fibroblast), "myogenic transdifferentiated cells" (3D_MyoD),
351 "adipogenic transdifferentiated cells" (3D+FI), and "myogenic/adipogenic
352 transdifferentiated cells" (3D_MyoD+FI) (Figure 8A). The Principle Component
353 Analysis (PCA) of the transcriptomes showed that distinct trajectories of myogenic and
354 adipogenic transdifferentiation routes were derived from the original fibroblasts and
355 finally integrated together into the myogenic/adipogenic cells (3D) (Figure 8B). It
356 indicates that the myogenic and adipogenic signalings could operate simultaneously
357 and separately during the generation of the culture meat with tunable fat content. The
358 heat map also highlighted the representative myogenic or adipogenic genes that were
359 upregulated in the myogenic, adipogenic, or myogenic/adipogenic cells constitute the
360 culture meat. In contrast, the fibroblast genes were diminished during the
361 transdifferentiation, confirming the loss of fibroblast identity (Figure 8C). In addition,
362 the Gene Ontology (GO) analysis of up-regulated differentially expressed genes (DEGs)
363 in 3D_MyoD+FI cells confirmed that myogenic-specific pathways such as "muscle
364 organ development" and adipogenic-specific pathways such as "PPAR signaling
365 pathway" were enriched. In addition, we also identified several multifunctional
366 signaling pathways such as "JAK-STAT signaling pathway", "NF-kappa B signaling
367 pathway", "MAPK signaling pathway" were simultaneously activated during
368 myogenic/adipogenic transdifferentiation, which should have profound effects on both
369 myogenesis(Bakkar and Guttridge, 2010; Jang and Baik, 2013; Keren et al., 2006) and

370 adipogensis (Batista et al., 2012; Bost et al., 2005; Richard and Stephens, 2011) (Figure
371 8D). The upregulated genes in the representative pathways (such as "*Stat1*" in JAK-
372 STAT signaling pathway, "*Mapkapk3*" in MAPK signaling pathway) were shown in
373 Figure 8E. In conclusion, the transcriptome analysis of the different types of
374 transdifferentiated cells revealed not only the myogenic- and adipogenic-specific
375 pathways driving the muscle formation and fat deposition respectively, but also several
376 key multifunctional signaling pathways that can promote the cell fate transition and
377 differentiation in different cellular contexts including the muscle and fat tissues.
378

Discussion

Mature muscle tissue primarily consists of myofibers (myotubes), which are long, multinucleated cells that contract to generate force and movement. In addition to myofibers, muscle tissue contains a variety of other cell types, including fibroblasts and adipocytes, all of which play important roles in the structure and function of the tissue. The extracellular matrix, which is mainly secreted by fibroblast cells, provides support and structural integrity to the muscle tissue. It is made up of a complex network of proteins and molecules, such as collagen, that provide a scaffold for the cells to attach to and interact with (Franco-Barraza et al., 2016). Together, these components contribute to the unique features of the skeletal muscle tissue and the fresh meat, including its strength, flexibility, and elasticity. It has been and still is challenging to recreate those characteristics in an in vitro condition of cultured meat production. One of the main obstacles in this process is the co-culturing of different cell types with distinct properties. In this study, we overcame this limitation of co-culturing different types of cells by utilizing a single source cell to generate various meat components, including muscle, fat and collagen. Precisely, we employed chicken fibroblasts to produce muscle, deposit fat, and synthesize collagen in a well-regulated and adjustable manner within a 3D setting to produce meat with desirable characteristics.

Fibroblasts are the one of the most common cell types in the animal and could serve as the seed cell for cultured meat production due to their unique and versatile features. First, the fibroblast cells are widely available in the bodies of agricultural animals and could be easily isolated and cultured in vitro. Second, many groups have successfully transformed the chicken fibroblasts into immortalized cell lines (Himly et al., 1998; Pasitka et al., 2023). These cell lines can provide an unlimited cellular resource for cultured meat production and eliminate the need for animal or embryo harvest. Third, fibroblasts are capable of adapting to low serum concentration medium or even serum-free medium, which greatly reduce the culturing cost and risk of serum-bound pathogens (Genbacev et al., 2005; Lohr et al., 2009; Pasitka et al., 2023). Last, the fibroblast cells can also undergo transformation to enable high-density propagation in suspension culture (Bürgin et al., 2020; Fluri et al., 2012; Shittu et al., 2016), which is a crucial step towards scaling up to mass-production. The Food and Drug Administration (FDA) has already approved the use of chicken fibroblast cells for cultured meat production and recently, Eat Just successfully utilized chicken fibroblasts for the commercial production and sale of cultured meat in Singapore (FDA, 2023).

One latest study has also demonstrated the feasibility and consumer acceptance of cultured meat derived solely from native chicken fibroblast cells, indicating a very promising development. However, the resulting meat products do not seem to contain any muscle components (Pasitka et al., 2023). We have previously established an effective strategy for myogenic transdifferentiation, allowing for the production of muscle cells from cultured fibroblast cells of various species in 2D culture (Ren et al., 2022). In the present study, we further enhanced the myogenic transdifferentiation process in 3D, and simultaneously simulated the fat deposition to create cell-based meat that more closely resembles real meat. As a proof-of-concept, we still utilized the transgene method and the final product still retains the foreign transgene fragment in the cells' genome. In the next step, other non-transgenic means such as non-integrating vectors, chemical reprogramming and recombinant transgene removal techniques will be explored to develop transgene-free products.

Numerous studies have identified the crucial role of fat in the aroma, juiciness, and tenderness of meat. In general, a very low level of intramuscular fat results in dry meat with plain taste, whereas the high intramuscular fat contents can improve the cooking flavor and greatly increase the value of meat products, such as the high marbling beef from Japanese Wagyu cattle (Gotoh et al., 2018; Motoyama et al., 2016). The fat content of fresh meat mainly come from lipids contained in the fat cells. Thus, closely mimicking the intramuscular fat properties in cultured meat would require co-culturing of muscle cells with fat cells. For example, co-culturing pre-adipocytes with myoblasts may increase the intramuscular fat content, tenderness, and taste intensity of cultured meat (Lau et al., 1996; Pandurangan and Kim, 2015; Zagury et al., 2022). However, co-culture of different cell types is technically challenging, since each cell type grows and differentiates in specific optimized medium. When different cell types are cultured in the same medium, these culture conditions may be sub-optimal for one cell type or the other and result in inefficient cellular growth (Pallaoro et al., 2023). Previous studies have underlined the influence adipocytes growing near muscle cells can impair myogenesis (Seo et al., 2019; Takegahara et al., 2014). Simultaneously or sequentially induction of both myogenic and lipogenic differentiation in the same starting seed cells would resolve these co-culture conflicts and the multi-lineage competent chicken fibroblast cells were chosen to explore this double transdifferentiation strategy. As a proof-of-concept study, we successfully transformed chicken fibroblast cells into muscle cells and deposited fat into the same cells in 3D hydrogel matrix. Notably, the

449 intramuscular fat content in the cultured meat could be tailored to any specific value
450 within a certain range. From a nutritional point of view, a direct comparison with the
451 traditional chicken meat was performed. The triglyceride content in the cultured meat
452 is comparable to that of chicken meat and more importantly, the amount of fat could be
453 easily manipulated in order to achieve a more attractive nutritional profile.
454
455 In this study, the fat deposition in the myotubes/myofibers enable the storage of large
456 amounts of lipids in muscle cells (intramuscular) but not in adipocytes (intermuscular)
457 of cultured meat. At present, we don't know if the fatty acids profile would be different
458 between the two types of origins. The unsaturated fats are conventionally regarded as
459 'healthier' than saturated fats (Berglund et al., 2007; Hamley, 2017). One of the superior
460 assets of cultured meat production is the ability to increase the unsaturated fat levels by
461 adjusting the additive fatty acids, oleic/linoleic acids in this case, in the culture medium.
462 In the future, it requires further comprehensive analysis of the fatty acids profile in the
463 cultured meat to elucidate the fat-associated attributes similar or distinct to real meat.
464
465 The current transcriptome analysis during the cellular transdifferentiation also revealed
466 key regulatory signaling pathways control the formation of cultured meat derived from
467 fibroblasts. Notably, we found several multi-functional pathways such as JAK-STAT,
468 MAPK signaling pathways were significantly enriched in the final cells underwent
469 double myogenic/adipogenic transdifferentiation. These signalings could drive the
470 differentiation process of many different types of cells including muscle and adipose
471 tissues (Bost et al., 2005; Jang and Baik, 2013; Keren et al., 2006; Richard and Stephens,
472 2011), and may be manipulated in current settings to further improve the generation of
473 final cultured meat with tunable fat content.
474
475 In conclusion, we have successfully used the immortalized chicken fibroblasts combine
476 with the 3D hydrogel to produce a cultured meat model that could precisely control the
477 synthesis of major components of the regular meat: muscle, fat and collagen. This
478 approach offers potential paths to the mass production of customized and versatile meat
479 which potentially being more attractive for different consumers.
480
481 **Materials and Methods**
482 **Cell preparation and inducible myogenic transdifferentiation**

483 The transdifferentiation cells were constructed as described previously (Ren et al.,
484 2022). Briefly, we cloned the chicken full MyoD coding sequence into a DOX-inducible
485 lentiviral system (Tet-On-MyoD). The wild-type chicken fibroblasts were deal with
486 viral infection and puromycin selection (Invivogen, #ant-pr-1), and finally obtained the
487 transdifferentiation cell lines. In addition, myofibroblasts were isolated from the skin
488 of 10-day-old chicken embryos in the same way as in the previous study (Kosla et al.,
489 2013). Cells were cultured in a 1640 basal medium (Gibco, #C11875500BT)
490 supplemented with 12% fetal bovine serum (FBS) (Gibco, #10270-106) and 1%
491 penicillin-streptomycin (Gibco, #11140050) at 39°C under 5% CO_2 atmosphere and
492 were given fresh medium every two days. When grown to approximately 80%
493 confluence, the cells were trypsinized and passaged.
494
495 **Domestication of cells in low concentration serum medium**
496 The chicken fibroblast cells were domesticated with the progressive concentration of
497 serum. In general, cells were cultured with 12% FBS in a 1640 basal medium and when
498 grown to about 80% confluence, the medium was replaced with 6% FBS medium for
499 further cell culture and passage. The medium was then changed to 3% FBS medium for
500 further cell culture and passage depending on the cell status, and so on. Start again and
501 repeat above steps as soon as the cells grow badly or die. We directly changed the cell
502 culture medium from 12% FBS to 2% CS then reduced it to 1% CS when using chicken
503 serum (CS) (Solarbio, #S9080) medium and the cells could adapt to the medium with
504 low concentration of chicken serum after 3-5 passages.
505
506 **Preparation of 3D scaffold and cell culture in 3D matirx**
507 GelMA hydrogels were purchased from Beijing ShangPu for this experiment. Weigh
508 the appropriate amount of GelMA powder into 1640 basal medium, dissolve in a water
509 bath at 70°C for about 30 min, and then filter with 0.22μm sieve. Add 1/8 volume of
510 lithium acylphosphinate salt photoinitiator to the dissolution solution to obtain GelMA
511 hydrogel solution, store at 37°C until usage but no more than 24 h. Fibroblast cells were
512 obtained by trypsin treatment and suspended with GelMA hydrogel solution and gently
513 mixed, followed by treatment of 405nm UV light for 10-20 s to get a 3D hydrogel
514 scaffold. In addition, the hydrogel is secured on a fixation ring for better cell growth
515 and easy movement (Figure S8A and S8B). Place the cell hydrogel complexes in 24-
516 well plate and culture with 1640 medium containing 12%FBS. Transferred to a new
517 well after 12 h, fresh medium was added and changed every 24 h. The cell hydrogel

518 complexes were gently washed three times with PBS buffer and digested by joining
519 collagen II enzyme (Sigma, #10270-106) in incubator at 39°C for 6 min until the cells
520 in the hydrogel package become rounding and shedding. Terminate digest by adding
521 medium and then centrifuged at 1,000 g for 10 min at room temperature (25°C).
522
523 **Cell Counting Kit-8 Assay**
524 Cells cultured in 1% CS and 12% FBS were seeded into 96-well plates with 100 μL of
525 medium per well and incubated for 0 h, 24 h, 48 h and 72 h. 10 μL of the cell Counting
526 Kit-8 Assay (CCK-8) solution (Solarbio, #CA1210, China) was then added to each well
527 and incubated for 2 h. The absorbance values at 450 nm were measured by an EnSpire
528 multifunctional spectrophotometer (Perkin Elmer, USA).
529
530 **EdU assay**
531 2D cells were cultured in 6-well plates, and 1 mL of the growth medium was added to
532 each well with 0.25 μL of 1.25 mg/mL 5-Ethynyl-2'-deoxyuridine (EdU) (Beyotime,
533 #ST067-1g). After 30 min of incubation, cells were fixed by 4% paraformaldehyde
534 (PFA) for 30 min. Cells were stained with a prepared reaction solution consisting of
535 1:100 $CuSO_4$, 1:4 Tris-HCl, 0.017 g/mL ascorbic acid, 1:1000 Alexa Fluor555 dye and
536 pure water. After 30 min, wash it with PBS, and the nuclei were stained with 50 ng/mL
537 DAPI for 10 min. 3D cultures of cells were cultured in 24-well plate dishes by adding
538 1mL of the medium with 0.25μL EdU, incubated for 1 h and then fixed with 4% PFA
539 for 24 h. Staining time extended to 1 h and nuclear staining 20 min. Fluorescence
540 images were collected using fluorescence microscopy.
541
542 **Cell differentiation**
543 For fibroblast induction into myoblasts, 50ng/ml DOX (Sigma, #D3000000) in 1640
544 basal medium containing 12% FBS was added for 3 days and the differentiation
545 medium was replaced when the cells reached 80% fusion. In addition, in 3D culture,
546 cells are proliferated for 7 days before changing the differentiation medium when a
547 dense arrangement of cells can be observed under the microscope.
548 For induction of lipogenic differentiation, the differentiation medium was changed
549 when the fusion rate of cells reached 80% in 2D culture or proliferated for 5 to 7 days
550 in 3D culture. The lipogenesis induction was for 48h with fresh medium changes every
551 24h. For the differentiation experiments, 1640 with 12% FBS was used as a control,
552 and the lipogenic medium was consistent with a 1:100 fatty acid ('F' for short)

553 composition of 1:1 oleic acid (Sigma, #O3008, 2 mol oleic acid/mole albumin) and
554 linoleic acids (Sigma, #L9530, 2 mol linoleic acid/mole albumin; 100 mg/mL albumin),
555 and insulin ('I' for short) (Sigma, #I0516) concentration of 60 μg/mL.
556
557 **Immunofluorescence staining**
558 Similar as our previous steps for immunofluorescence staining of cells in 2D culture
559 (Luo et al., 2022), cells were fixed in 4% PFA for 30 min and washed three times with
560 PBS buffer at room temperature, then permeabilizing with 0.5% Triton X-100 on PBS
561 for 10 min and blocking with 10% goat serum at 0.5% TritonX-100 for 1 h. Primary
562 antibodies were diluted with 10% goat serum in 0.5% Triton X-100 at 4°C for 12 h. The
563 primary antibody for MHC (DSHB, #AB2147781) and the primary antibody for
564 Desmin (Sigma, #D8281) were added at a dilution of 1:500 and the primary antibody
565 for Vimentin (DSHB, #AB528504) at a dilution of 1:200. Followed by incubation with
566 Alexa secondary antibody (Invitrogen, #A-21202, #A-21206 and #A-31570) at a 1:500
567 dilution for 2 h at room temperature. Antibody for α-SMA (Sigma, C6198) was added
568 at a dilution of 1:500 and incubated with 10% goat serum in 0.5% Triton X-100 at room
569 temperature for 2h. Nuclear staining was performed with 50 ng/mL DAPI (Sigma,
570 #D8417) for 10 min. Cells in the 3D culture were fixed for 48 h, the total time of
571 permeabilizing and the blocking was no more than 24 h, and the incubation time of the
572 primary antibody was extended to 24 h, the secondary antibody was 4 h and the nuclear
573 staining 20 min. For MHC detection, fluorescence images were collected using
574 fluorescence microscopy and the $MHC^{+}DAPI^{+}/DAPI^{+}$ differentiation index was
575 calculated from three or more images using confocal microscopy (Zeiss LSM 800).
576
577 **Oil Red O Staining**
578 For Oil Red O staining, cells were fixed with 4% PFA for 30 min or 24 h respectively
579 in 2D and 3D culture. After washing thrice with PBS at room temperature, the cells
580 were soaked in 60% isopropanol for better coloration of Oil Red and then washed for 5
581 min or 10 min respectively in 2D and 3D culture. The cells were stained with Oil Red
582 O (Sigma, #O0625) for 30 min or 60 min respectively in 2D and 3D. Cells were washed
583 with 60% isopropanol for 30 s or 1 min respectively in 2D and 3D to remove surface
584 staining. Then, cells were washed with distilled water for three times and the stained
585 lipid droplets were visualized using a microscope.
586

587 **mRNA extraction and real-time quantitative PCR (qPCR) and library**
588 **construction**
589 Cells were lysed in Trizol (Simgen, #5301100) and RNA was extracted following
590 manufacture's recommendations. RNA concentration was measured on NanoDrop2000
591 (Thermo Scientific, USA). 1 μg of RNA was reverse transcribed using PrimeScriptTM
592 RT reagent Kit (Takara, #RR047A). Real-time quantitative PCR was performed using
593 SYBR Green Mix (Abclonal, #RK21203) following manufacturer's instructions.
594 Expression was normalized to GAPDH using delta-delta-CT method. For comparisons
595 of the expression, we used a one-tailed Student's t-test. The error bars indicate the SEM.
596 The RT-qPCR primers are described in Table S1. The RNA-Seq library-preparation
597 protocol was based on the NEBNext Ultra™ RNA Library Prep Kit for Illumina (NEB,
598 #E7530L). Insert size was assessed using the Agilent Bioanalyzer 2100 system and
599 qualified insert size was accurate quantification using StepOnePlus™ Real-Time PCR
600 System (Library valid concentration＞10nM) and then paired-end sequencing using an
601 Illumina platform. RNA-Seq was performed on triplicates for each sample.
602
603 **RNA-Seq data analysis**
604 The RNA-Seq raw data were firstly trimmed adapters by trim_galore software (Bolger
605 et al., 2014) and then the clean data of RNA-Seq was mapped to chicken genome
606 (Ensembl, GRCg7b) using hisat2 (Kim et al., 2019) with default parameters. Because
607 of using paired-end reads, the concordant unique mapping reads/pairs were kept based
608 on the mapping flags. The duplications were removed based on the coordinates of the
609 reads/pairs. The de-duplication unique mapping reads/pairs were used for further
610 analysis in this study. Read counts for each sample were computed with the
611 featureCounts (Liao et al., 2014) software and the RefSeq gene annotation for chicken
612 genome assembly is GRCg7b. The transcript per million (TPM) were normalized using
613 reads counts. Differential expressed genes (DEGs) of RNA-Seq data were analyzed
614 using DESeq2 called by $q<0.01$ and fold change >2 thresholds. The chicken genes were
615 transformed to homologue human genes using ensemble bioMart database and the gene
616 ontology in this study was conducted in Metascape and the enriched top pathways were
617 shown. All plots were generated by R (v4.0.3).
618
619 **Measurement of total collagen content in cultured meat**
620 Total collagen content was determined by the concentration of hydroxyproline. The
621 medium was replaced with fresh medium in the incubator for 2 h before the assay,

washed three times with PBS. According to the instructions of the Hydroxyproline Assay Kit (Jiancheng, #A030-1-1, China), one volume of saline was added in dried cultured meat at a 1:1 ratio of weight and volume. After mechanical homogenization in ice-water bath, the digestion solution was incubated at 37°C in a water bath for 4 h. Hydroxyproline content was measured by the absorbance at 550 nm using an EnSpire multifunctional spectrophotometer (Perkin Elmer, USA). For each measurement of cultured meat, the hydroxyproline content of the corresponding blank cell-free hydrogel was substracted. The amount of collagen was calculated from the hydroxyproline concentration with a conversion factor of 7.25 in μg/mg wet tissue (Vasanthi et al., 2007; Zheng et al., 2021).

Measurement of triglyceride content in cultured meat

The triglyceride content in cultured meat was measured using the kit (Solarbio, #BC0620, China). Before the assay, the culture system is washed three times with PBS and uniformly added to the same medium containing 12% FBS in the incubator for 2 h, after which it is removed and washed three more times with PBS, the cultured meat is taken out and churned, and the precipitate is obtained by centrifugation, which should be well air-dried. The precipitate was weighed and tirzol was added to lyse well for 2 h. A mixture of n-heptane and isopropanol in a ratio of 1:1 was then added and shaken and mixed. Then added potassium hydroxide and full shaken to produce glycerol and fatty acids, then the other reagents were added in sequence according to the instructions. The final triglyceride content was measured the specific light intensity at 420 nm, as described previously.

Emission scanning electron microscope

The cell hydrogels were washed three times with PBS and then fixed in 4% PFA for 1 h. Samples were randomly clamped into spiking trays, rapidly frozen in liquid nitrogen and then images were randomly collected using the emission scanning electron microscope (HITACHI SU8010, Japan).

Statistical analyses

Statistical analyses were performed using the Graph-Pad Prism software. For normally distributed data sets with equal variances, a two-sample t-test was used. The significance of differences was provided in figure legends.

Acknowledgements

This work was supported by National Natural Science Foundation of China (31771617) and Taishan Scholar Program.

661 **References**

662 Addison, W.N., Fu, M.M., Yang, H.X., Lin, Z., Nagano, K., Gori, F., and Baron, R. (2014). Direct
663 transcriptional repression of Zfp423 by Zfp521 mediates a bone morphogenic protein-dependent
664 osteoblast versus adipocyte lineage commitment switch. Mol Cell Biol *34*, 3076-3085.
665 Bakkar, N., and Guttridge, D.C. (2010). NF-kappaB signaling: a tale of two pathways in skeletal
666 myogenesis. Physiological reviews *90*, 495-511.
667 Batista, M.L., Jr., Peres, S.B., McDonald, M.E., Alcantara, P.S., Olivan, M., Otoch, J.P., Farmer, S.R.,
668 and Seelaender, M. (2012). Adipose tissue inflammation and cancer cachexia: possible role of nuclear
669 transcription factors. Cytokine *57*, 9-16.
670 Ben-Arye, T., and Levenberg, S. (2019). Tissue Engineering for Clean Meat Production. Frontiers in
671 Sustainable Food Systems *3*.
672 Berglund, L., Lefevre, M., Ginsberg, H.N., Kris-Etherton, P.M., Elmer, P.J., Stewart, P.W., Ershow, A.,
673 Pearson, T.A., Dennis, B.H., Roheim, P.S.*, et al.* (2007). Comparison of monounsaturated fat with
674 carbohydrates as a replacement for saturated fat in subjects with a high metabolic risk profile: studies in
675 the fasting and postprandial states. Am J Clin Nutr *86*, 1611-1620.
676 Bolger, A.M., Lohse, M., and Usadel, B. (2014). Trimmomatic: a flexible trimmer for Illumina sequence
677 data. Bioinformatics (Oxford, England) *30*, 2114-2120.
678 Bost, F., Aouadi, M., Caron, L., and Binétruy, B. (2005). The role of MAPKs in adipocyte differentiation
679 and obesity. Biochimie *87*, 51-56.
680 Bürgin, T., Coronel, J., Hagens, G., Keebler, M.V., Genzel, Y., Reichl, U., and Anderlei, T. (2020).
681 Orbitally Shaken Single-Use Bioreactor for Animal Cell Cultivation: Fed-Batch and Perfusion Mode.
682 Methods Mol Biol *2095*, 105-123.
683 Cao, Y., Kumar, R.M., Penn, B.H., Berkes, C.A., Kooperberg, C., Boyer, L.A., Young, R.A., and Tapscott,
684 S.J. (2006). Global and gene-specific analyses show distinct roles for Myod and Myog at a common set
685 of promoters. Embo J *25*, 502-511.
686 Chriki, S., and Hocquette, J.F. (2020). The Myth of Cultured Meat: A Review. Frontiers in Nutrition *7*.
687 Fluri, D.A., Tonge, P.D., Song, H., Baptista, R.P., Shakiba, N., Shukla, S., Clarke, G., Nagy, A., and
688 Zandstra, P.W. (2012). Derivation, expansion and differentiation of induced pluripotent stem cells in
689 continuous suspension cultures. Nat Methods *9*, 509-516.
690 Franco-Barraza, J., Beacham, D.A., Amatangelo, M.D., and Cukierman, E. (2016). Preparation of
691 Extracellular Matrices Produced by Cultured and Primary Fibroblasts. Curr Protoc Cell Biol *71*,
692 10.19.11-10.19.34.
693 Frank, D., Ball, A., Hughes, J., Krishnamurthy, R., Piyasiri, U., Stark, J., Watkins, P., and Warner, R.
694 (2016). Sensory and Flavor Chemistry Characteristics of Australian Beef: Influence of Intramuscular Fat,
695 Feed, and Breed. J Agric Food Chem *64*, 4299-4311.
696 French, M.M., Rose, S., Canseco, J., and Athanasiou, K.A. (2004). Chondrogenic differentiation of adult
697 dermal fibroblasts. Ann Biomed Eng *32*, 50-56.
698 Genbacev, O., Krtolica, A., Zdravkovic, T., Brunette, E., Powell, S., Nath, A., Caceres, E., McMaster, M.,
699 McDonagh, S., Li, Y.*, et al.* (2005). Serum-free derivation of human embryonic stem cell lines on human
700 placental fibroblast feeders. Fertil Steril *83*, 1517-1529.
701 Gotoh, T., Nishimura, T., Kuchida, K., and Mannen, H. (2018). The Japanese Wagyu beef industry:
702 current situation and future prospects - A review. Asian-Australas J Anim Sci *31*, 933-950.
703 Hamley, S. (2017). The effect of replacing saturated fat with mostly n-6 polyunsaturated fat on coronary
704 heart disease: a meta-analysis of randomised controlled trials. Nutr J *16*, 30.

Hausman, G.J. (2012). MEAT SCIENCE AND MUSCLE BIOLOGY SYMPOSIUM: The influence of extracellular matrix on intramuscular and extramuscular adipogenesis. J Anim Sci *90*, 942-949.

Hecker, L., Jagirdar, R., Jin, T., and Thannickal, V.J. (2011). Reversible differentiation of myofibroblasts by MyoD. Exp Cell Res *317*, 1914-1921.

Himly, M., Foster, D.N., Bottoli, I., Iacovoni, J.S., and Vogt, P.K. (1998). The DF-1 chicken fibroblast cell line: Transformation induced by diverse oncogenes and cell death resulting from infection by avian leukosis viruses. Virology *248*, 295-304.

Hinz, B., Phan, S.H., Thannickal, V.J., Galli, A., Bochaton-Piallat, M.L., and Gabbiani, G. (2007). The myofibroblast: one function, multiple origins. Am J Pathol *170*, 1807-1816.

Jang, Y.N., and Baik, E.J. (2013). JAK-STAT pathway and myogenic differentiation. Jak-stat *2*, e23282.

Jeong, D., Seo, J.W., Lee, H.G., Jung, W.K., Park, Y.H., and Bae, H. (2022). Efficient Myogenic/Adipogenic Transdifferentiation of Bovine Fibroblasts in a 3D Bioprinting System for Steak-Type Cultured Meat Production. Adv Sci *9*.

Keren, A., Tamir, Y., and Bengal, E. (2006). The p38 MAPK signaling pathway: a major regulator of skeletal muscle development. Molecular and cellular endocrinology *252*, 224-230.

Kim, D., Paggi, J.M., Park, C., Bennett, C., and Salzberg, S.L. (2019). Graph-based genome alignment and genotyping with HISAT2 and HISAT-genotype. Nature biotechnology *37*, 907-915.

Kim, D.H., Lee, J., Suh, Y., Cressman, M., and Lee, K. (2021). Research Note: Adipogenic differentiation of embryonic fibroblasts of chicken, turkey, duck, and quail in vitro by medium containing chicken serum alone. Poultry Sci *100*.

Kim, D.H., Lee, J., Suh, Y., Cressman, M., Lee, S.S., and Lee, K. (2020). Adipogenic and Myogenic Potentials of Chicken Embryonic Fibroblasts in vitro: Combination of Fatty Acids and Insulin Induces Adipogenesis. Lipids *55*, 163-171.

Kosla, J., Dvorak, M., and Cermak, V. (2013). Molecular analysis of the TGF-beta controlled gene expression program in chicken embryo dermal myofibroblasts. Gene *513*, 90-100.

Lau, D.C.W., Shillabeer, G., Li, Z.H., Wong, K.L., Varzaneh, F.E., and Tough, S.C. (1996). Paracrine interactions in adipose tissue development and growth. Int J Obesity *20*, S16-S25.

Lee, J., Kim, D.H., Suh, Y., and Lee, K. (2021). Research Note: Potential usage of DF-1 cell line as a new cell model for avian adipogenesis. Poultry Sci *100*.

Liao, Y., Smyth, G.K., and Shi, W. (2014). featureCounts: an efficient general purpose program for assigning sequence reads to genomic features. Bioinformatics (Oxford, England) *30*, 923-930.

Lohr, V., Rath, A., Genzel, Y., Jordan, I., Sandig, V., and Reichl, U. (2009). New avian suspension cell lines provide production of influenza virus and MVA in serum-free media: studies on growth, metabolism and virus propagation. Vaccine *27*, 4975-4982.

Longo, M., Raciti, G.A., Zatterale, F., Parrillo, L., Desiderio, A., Spinelli, R., Hammarstedt, A., Hedjazifar, S., Hoffmann, J.M., Nigro, C.*, et al.* (2018). Epigenetic modifications of the Zfp/ZNF423 gene control murine adipogenic commitment and are dysregulated in human hypertrophic obesity. Diabetologia *61*, 369-380.

Luo, W., Xu, Y., Liu, R., Liao, Y., Wang, S., Zhang, H., Li, X., and Wang, H. (2022). Retinoic acid and RARγ maintain satellite cell quiescence through regulation of translation initiation. Cell Death Dis *13*, 838.

Mattick, C.S., Landis, A.E., and Allenby, B.R. (2015). A case for systemic environmental analysis of cultured meat. Journal of Integrative Agriculture *14*, 249-254.

Motoyama, M., Sasaki, K., and Watanabe, A. (2016). Wagyu and the factors contributing to its beef

749 quality: A Japanese industry overview. Meat Sci *120*, 10-18.
750 Nakashima, K., Yamazaki, M., and Abe, H. (2005). Effects of serum deprivation on expression of
751 proteolytic-related genes in chick myotube cultures. Biosci Biotechnol Biochem *69*, 623-627.
752 Pallaoro, M., Modina, S.C., Fiorati, A., Altomare, L., Mirra, G., Scocco, P., and Di Giancamillo, A.
753 (2023). Towards a More Realistic In Vitro Meat: The Cross Talk between Adipose and Muscle Cells. Int
754 J Mol Sci *24*.
755 Pandurangan, M., and Kim, D.H. (2015). A novel approach for in vitro meat production. Appl Microbiol
756 Biot *99*, 5391-5395.
757 Pasitka, L., Cohen, M., Ehrlich, A., Gildor, B., Reuveni, E., Ayyash, M., Wissotsky, G., Herscovici, A.,
758 Kaminker, R., Niv, A.*, et al.* (2023). Spontaneous immortalization of chicken fibroblasts generates stable,
759 high-yield cell lines for serum-free production of cultured meat (Dec, 10.1038/s43016-022-00658-w,
760 2022). Nature Food *4*, 124-124.
761 Paulin, D., and Li, Z. (2004). Desmin: a major intermediate filament protein essential for the structural
762 integrity and function of muscle. Exp Cell Res *301*, 1-7.
763 Pepelanova, I., Kruppa, K., Scheper, T., and Lavrentieva, A. (2018). Gelatin-methacryloyl (GelMA)
764 hydrogels with defined degree of functionalization as a versatile toolkit for 3D cell culture and extrusion
765 bioprinting. Bioengineering *5*, 55.
766 Relaix, F., Demignon, J., Laclef, C., Pujol, J., Santolini, M., Niro, C., Lagha, M., Rocancourt, D.,
767 Buckingham, M., and Maire, P. (2013). Six homeoproteins directly activate Myod expression in the gene
768 regulatory networks that control early myogenesis. PLoS Genet *9*, e1003425.
769 Ren, R.M., Fan, Y., Peng, Z.L., Wang, S., Jiang, Y.Q., Fu, L.L., Cao, J.H., Zhao, S.H., and Wang, H.
770 (2022). Characterization and perturbation of CTCF-mediated chromatin interactions for enhancing
771 myogenic transdifferentiation. Cell Reports *40*.
772 Richard, A.J., and Stephens, J.M. (2011). Emerging roles of JAK-STAT signaling pathways in adipocytes.
773 Trends in endocrinology and metabolism: TEM *22*, 325-332.
774 Seo, K., Suzuki, T., Kobayashi, K., and Nishimura, T. (2019). Adipocytes suppress differentiation of
775 muscle cells in a co-culture system. Anim Sci J *90*, 423-434.
776 Shittu, I., Zhu, Z., Lu, Y., Hutcheson, J.M., Stice, S.L., West, F.D., Donadeu, M., Dungu, B., Fadly, A.M.,
777 Zavala, G.*, et al.* (2016). Development, characterization and optimization of a new suspension chicken-
778 induced pluripotent cell line for the production of Newcastle disease vaccine. Biologicals *44*, 24-32.
779 Takase, S., Leo, M.A., Nouchi, T., and Lieber, C.S. (1988). Desmin distinguishes cultured fat-storing
780 cells from myofibroblasts, smooth muscle cells and fibroblasts in the rat. J Hepatol *6*, 267-276.
781 Takegahara, Y., Yamanouchi, K., Nakamura, K., Nakano, S., and Nishihara, M. (2014). Myotube
782 formation is affected by adipogenic lineage cells in a cell-to-cell contact-independent manner. Exp Cell
783 Res *324*, 105-114.
784 Tarbit, E., Singh, I., Peart, J.N., and Rose'Meyer, R.B. (2019). Biomarkers for the identification of cardiac
785 fibroblast and myofibroblast cells. Heart Fail Rev *24*, 1-15.
786 van Rooij, E., Quiat, D., Johnson, B.A., Sutherland, L.B., Qi, X., Richardson, J.A., Kelm, R.J., Jr., and
787 Olson, E.N. (2009). A family of microRNAs encoded by myosin genes governs myosin expression and
788 muscle performance. Dev Cell *17*, 662-673.
789 Vasanthi, C., Venkataramanujam, V., and Dushyanthan, K. (2007). Effect of cooking temperature and
790 time on the physico-chemical, histological and sensory properties of female carabeef (buffalo) meat.
791 Meat Sci *76*, 274-280.
792 Vaughan, M.B., Howard, E.W., and Tomasek, J.J. (2000). Transforming growth factor-beta1 promotes

the morphological and functional differentiation of the myofibroblast. Exp Cell Res *257*, 180-189.

Vincent, C.K., Gualberto, A., Patel, C.V., and Walsh, K. (1993). Different regulatory sequences control creatine kinase-M gene expression in directly injected skeletal and cardiac muscle. Mol Cell Biol *13*, 1264-1272.

Warkman, A.S., Whitman, S.A., Miller, M.K., Garriock, R.J., Schwach, C.M., Gregorio, C.C., and Krieg, P.A. (2012). Developmental expression and cardiac transcriptional regulation of Myh7b, a third myosin heavy chain in the vertebrate heart. Cytoskeleton (Hoboken) *69*, 324-335.

Weintraub, H., Tapscott, S.J., Davis, R.L., Thayer, M.J., Adam, M.A., Lassar, A.B., and Miller, A.D. (1989). Activation of muscle-specific genes in pigment, nerve, fat, liver, and fibroblast cell lines by forced expression of MyoD. Proc Natl Acad Sci U S A *86*, 5434-5438.

Yin, J., Jin, X., Beck, S., Kang, D.H., Hong, Z., Li, Z., Jin, Y., Zhang, Q., Choi, Y.J., Kim, S.C.*, et al.* (2010). In vitro myogenic and adipogenic differentiation model of genetically engineered bovine embryonic fibroblast cell lines. Biotechnol Lett *32*, 195-202.

Zagury, Y., Ianovici, I., Landau, S., Lavon, N., and Levenberg, S. (2022). Engineered marble-like bovine fat tissue for cultured meat. Commun Biol *5*, 927.

Zheng, Y.Y., Zhu, H.Z., Wu, Z.Y., Song, W.J., Tang, C.B., Li, C.B., Ding, S.J., and Zhou, G.H. (2021). Evaluation of the effect of smooth muscle cells on the quality of cultured meat in a model for cultured meat. Food Res Int *150*, 110786.

812 **Figures and legends**

813

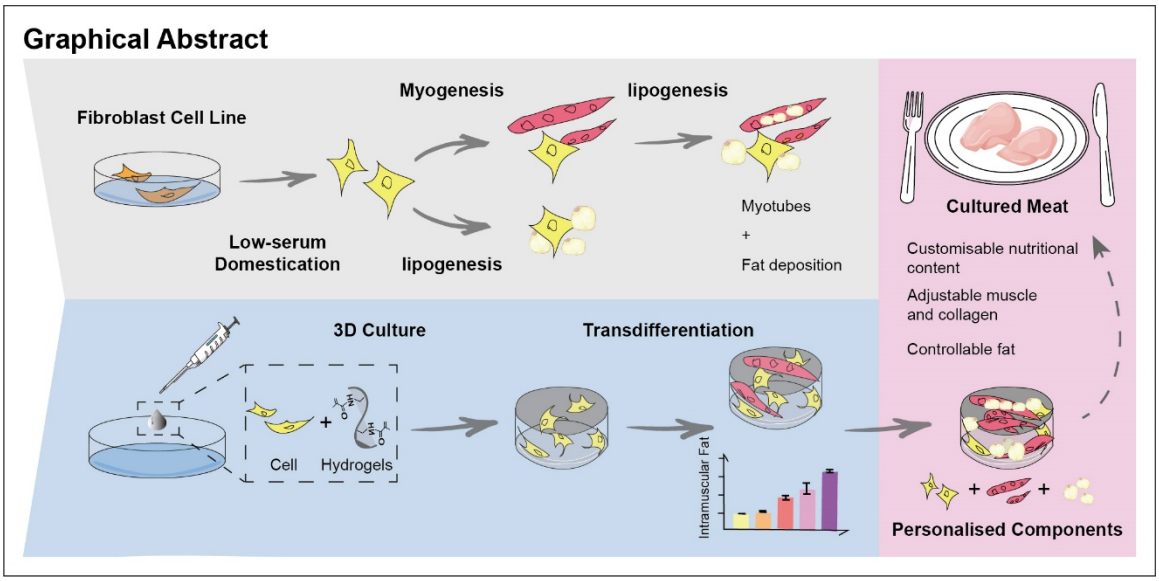

814

815 **Graphical abstract.**

816

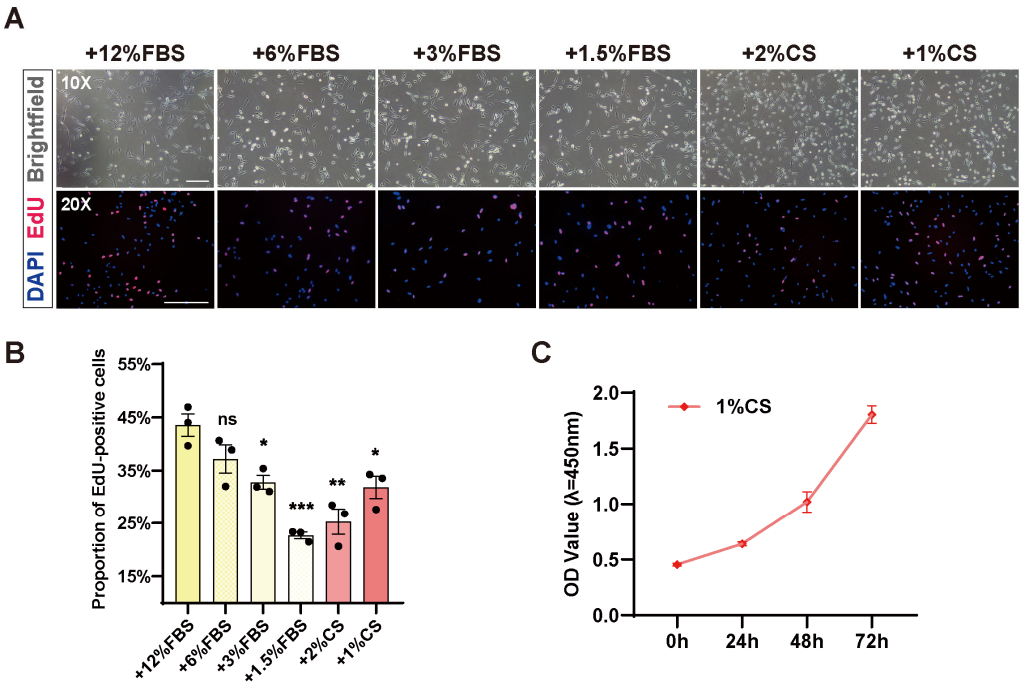

Figure 1. Chicken fibroblasts proliferate stably in low-serum conditions. (A) Cellular morphology and EdU staining of chicken fibroblasts under different low-serum conditions. FBS: Fetal bovine serum. CS: Chicken serum. Scale bar, 200 μm. (B) Quantification of the proportion of EdU-positive cells in Figure A. Error bars indicate s.e.m. (C) The CCK-8 cell proliferation assay showed the proliferation of chicken fibroblasts in 1% chicken serum. Error bars indicate s.e.m, n = 3.

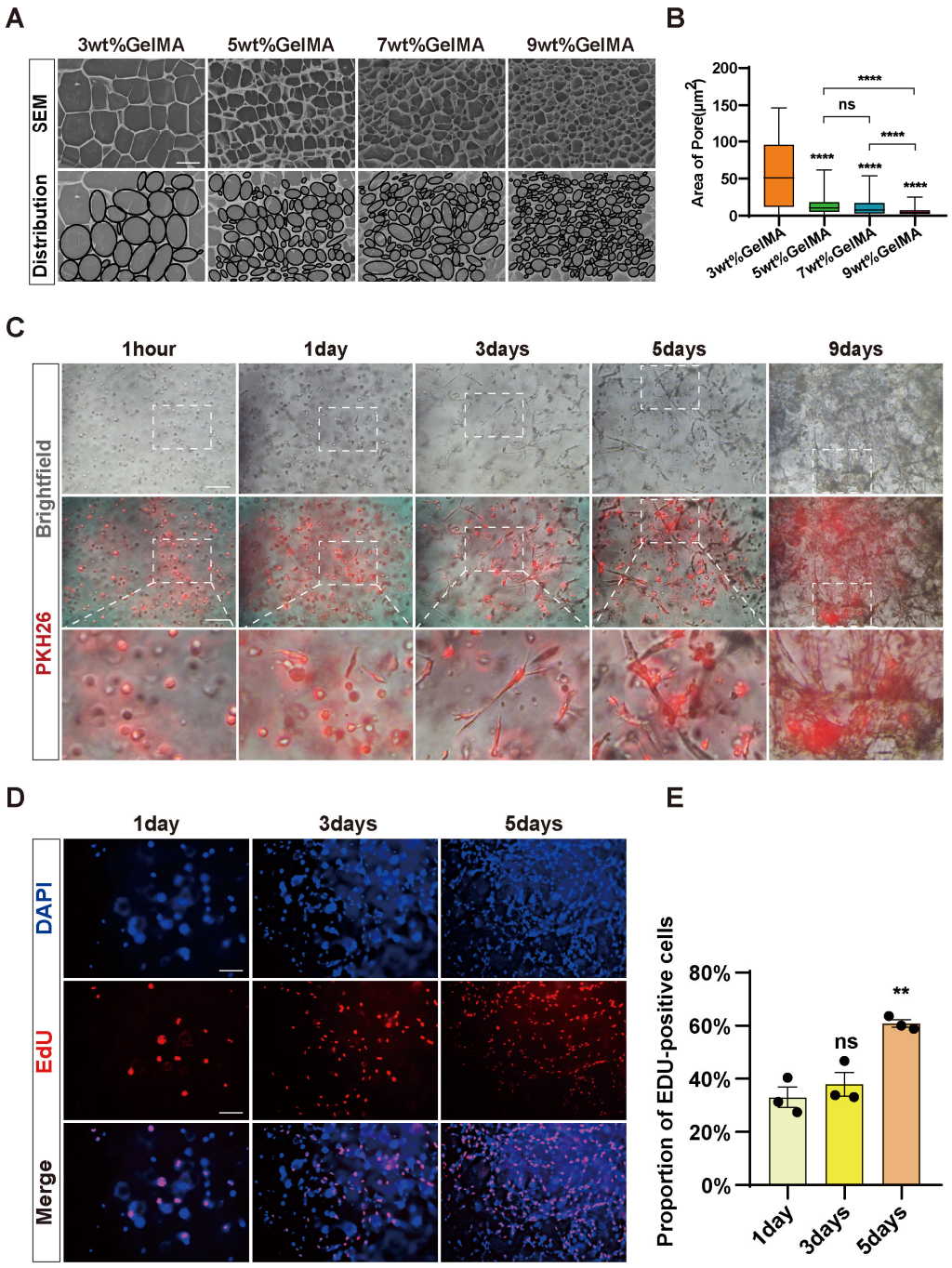

Figure 2. 3D culture of chicken fibroblasts in GelMA hydrogels. (A) Microscopic images of GelMA hydrogels at different concentrations (3%wt, 5%wt, 7%wt and 9%wt) taken by scanning electron microscopy and their corresponding simplified maps of pore distributions. Scale bar, 10 μm. (B) Quantification of pore area in image A. Error bars indicate s.e.m, n = 3. ****P < 0.0001. (C) Brightfield and red fluorescent images of

cells in 3D culture after PKH26 staining at different times (1hour, 1day, 3days, 5days and 9days). Scale bar, 100 μm. (D) Representative EdU staining shows the proliferation of cells in 3D culture on 1day, 3days and 5 days after cell implantation in hydrogel. Scale bar, 100 μm. (E) Quantification of the proportion of EdU-positive cells in Figure D. Error bars indicate s.e.m, n = 3. **$P < 0.01$.

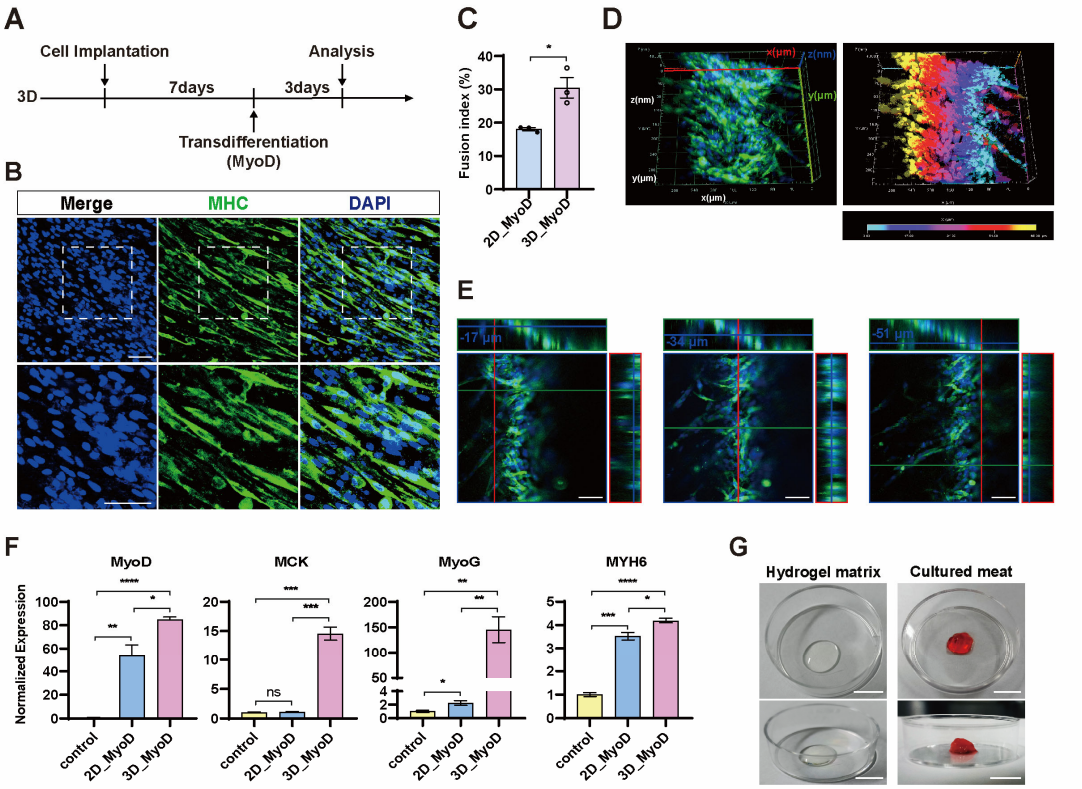

Figure 3. Transdifferentiation of chicken fibroblasts into muscle cells in 3D. (A) Experimental design for fibroblast myogenic transdifferentiation in 3D culture. (B) Representative images of MHC staining showed the myogenic ability of chicken fibroblasts in 3D culture. Scale bar, 50 μm. (C) Comparison of the mean myogenic fusion index between 2D and 3D. Error bars indicate s.e.m, n = 3. *P < 0.05. (D) Three-dimensional images of MHC staining of cells cultured in 3D. The right panel is its depth-coded image which indicate different depths from the deepest (cyan) to the surface (yellow). (E) Orthogonal projections of three sets of MHC staining of cells in 3D culture at different depths. Scale bar, 50 μm. (F) Expression of skeletal muscle-related genes was determined by RT-qPCR in 2D and 3D cells upon myogenic transdifferentiation and control 3D cells without stimulation. Please note that the myogenic transdifferentiation driven by MyoD stimulate the expression of classical myogenic factors. Error bars indicate s.e.m, n = 3. *P < 0.05, **P < 0.01, ***P < 0.001, ****P < 0.0001. (G) Macroscopic morphology of the empty hydrogel matrix (left) and cultured meat (right). The cultured meat is the product obtained after 3D cell culture and induction of myogenesis/lipogenesis. Scale bar, 1 cm.

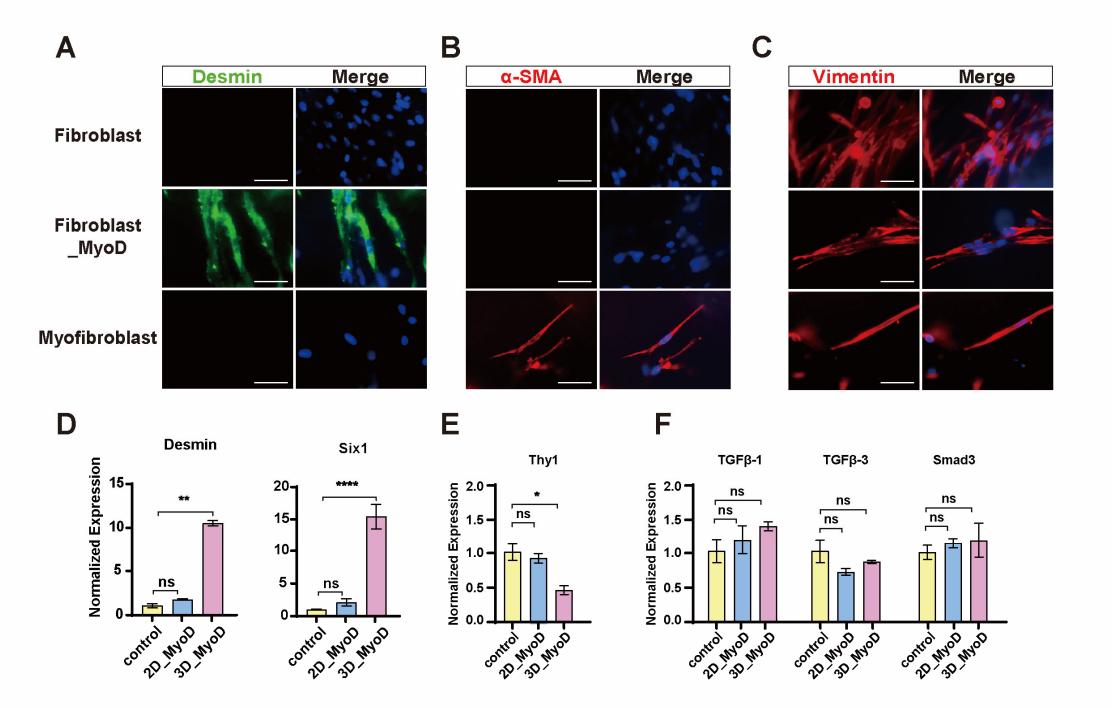

Figure 4. Myogenic transdifferentiation of fibroblasts do not produce myofibroblasts. (A) Immunofluorescence staining of 3D cultured cells showed that the skeletal muscle marker desmin was expressed only in the transdifferentiated cells but not in fibroblasts or myofibroblasts. Scale bar, 50 μm. (B) Immunofluorescence staining of 3D cultured cells showed that the myofibroblast marker α-SMA was expressed only in the myofibroblasts but not in fibroblasts or transdifferentiated cells. Scale bar, 50 μm. (C) Immunofluorescence staining of 3D cultured cells showed that the fibroblast marker vimentin was abundantly expressed in fibroblasts and myofibroblasts but greatly reduced in transdifferentiated cells. Scale bar, 50 μm. (D) RT-qPCR showed that the myogenic genes Desmin and Six1 were significantly increased upon myogenic transdifferentiation. (E) RT-qPCR showed the fibroblast marker gene Thy-1 was significantly reduced upon myogenic transdifferentiation. (F) The myofibroblast marker genes TGFβ-1, TGFβ-3 and Smad3 remain unchanged during myogenic transdifferentiation. Error bars indicate s.e.m, n = 4. *P < 0.05, **P < 0.01, ***P < 0.001, ****P < 0.0001. ns: not significant.

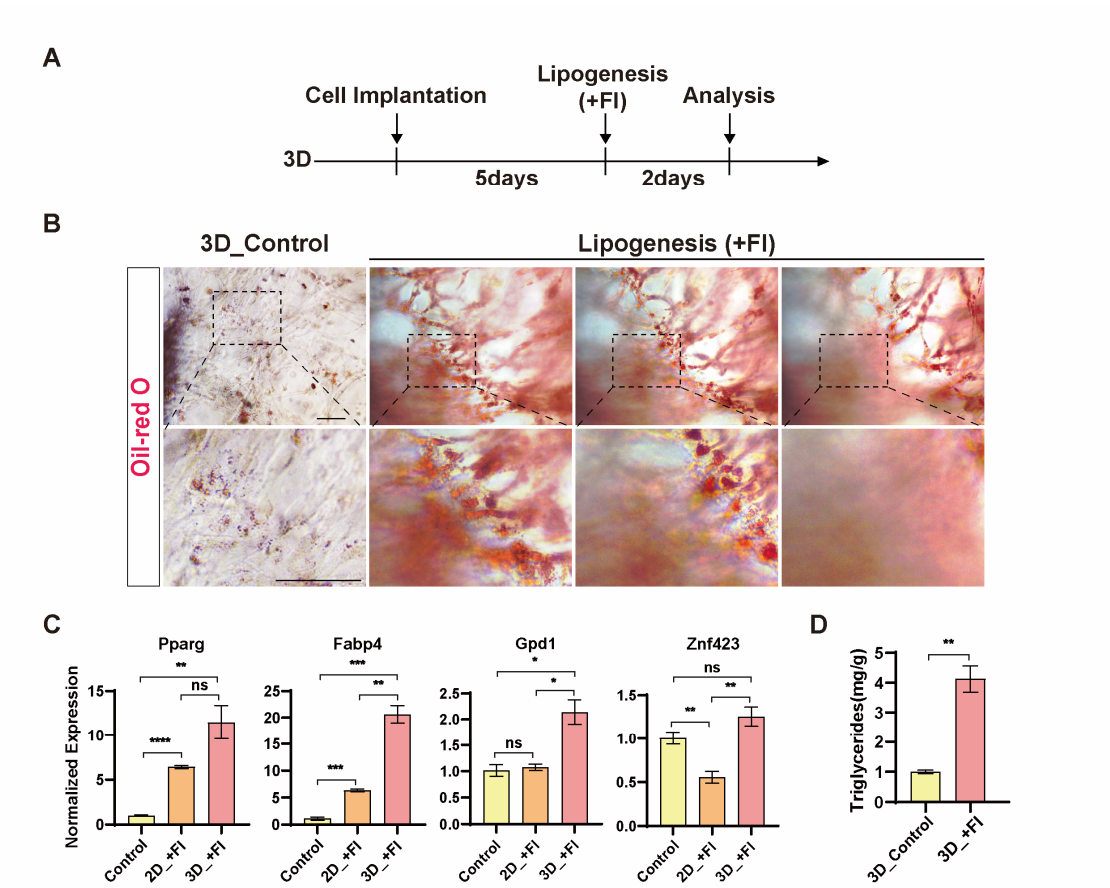

Figure 5. Stimulate the fat deposition in chicken fibroblasts in 3D. (A) Experimental design for fibroblast lipogenesis in 3D culture ('F' is for fatty acids and 'I' is for insulin). (B) Representative images showing the Oil-red O staining of lipid content accumulated in cells at different focal planes at the same position. The control group was normal medium without lipogenesis. Scale bar, 100 μm. (C) Expression of lipid synthesis related genes determined by RT-qPCR in 2D and 3D cells upon lipogenic induction and control 3D cells without stimulation. Error bars indicate s.e.m, n = 3. *P < 0.05, **P < 0.01, ***P < 0.001, ****P < 0.0001. (D) Triglyceride content in the cultured meat upon different lipogenic inductions and control 3D cells without stimulation. Error bars indicate s.e.m, n = 3. *P < 0.05, **P < 0.01, ***P < 0.001.

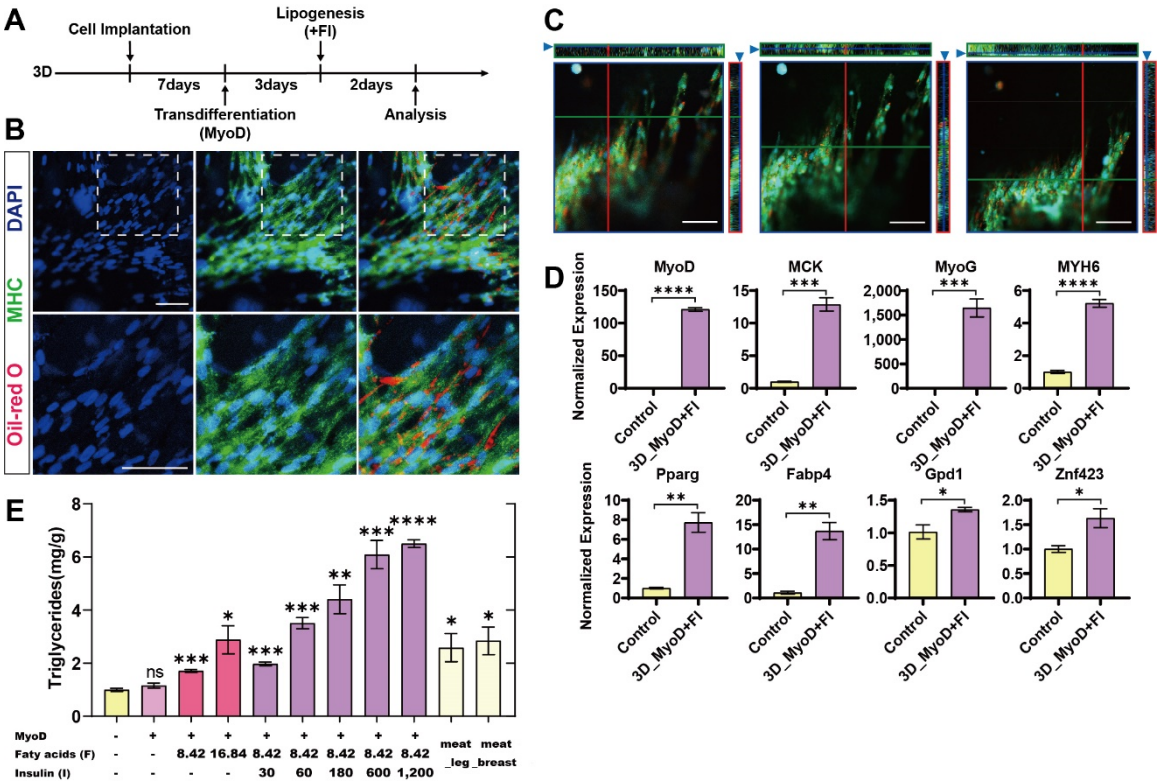

Figure 6. Controlled fat deposition in the transdifferentiated muscle cells in 3D hydrogel. (A) Experimental design for fibroblast myogenic/lipogenic differentiation in 3D culture. (B) Representative images of MHC and Oil Red O staining of cells upon myogenesis/lipogenesis in 3D culture. Scale bar, 50 µm. (C) Orthogonal projections of three sets of MHC and Oil Red O staining of cells in 3D culture at different depths. Scale bar, 50 µm. (D) Expression of muscle-related genes (top) and lipid-related genes (bottom) in the cells with myogenesis/lipogenesis induction and control 3D cells without any stimulation were determined by RT-qPCR. (E) Triglyceride content of cultured meat under different conditions and real meat. “Meat_leg” and “Meat_breast” are taken from the leg and breast muscles of adult chickens. Error bars indicate s.e.m, n = 3. *P < 0.05, **P < 0.01, ***P < 0.001, ****P < 0.0001.

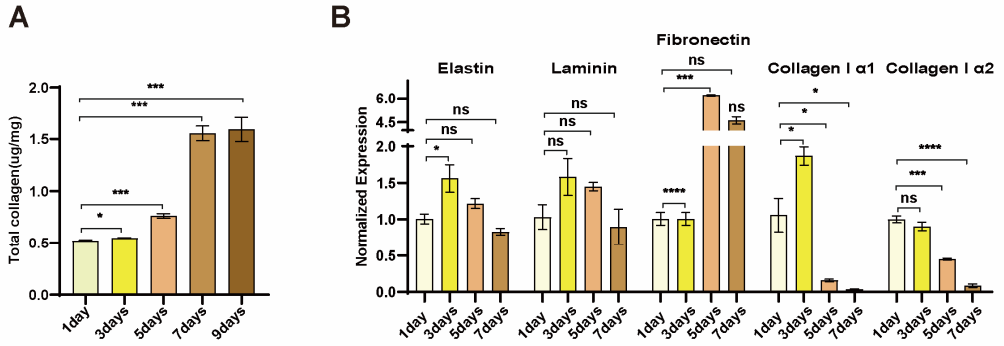

Figure 7. The collagen content and expression of ECM component genes in cultured meat. (A) Total collagen content of cultured meat at different days of cultivation. Error bars indicate s.e.m, n = 3. *P < 0.05, ***P < 0.001. (B) Expression of ECM-related genes determined by RT-qPCR of cultured meat. Error bars indicate s.e.m, n = 3. *P < 0.05, ***P < 0.001, ****P < 0.0001.

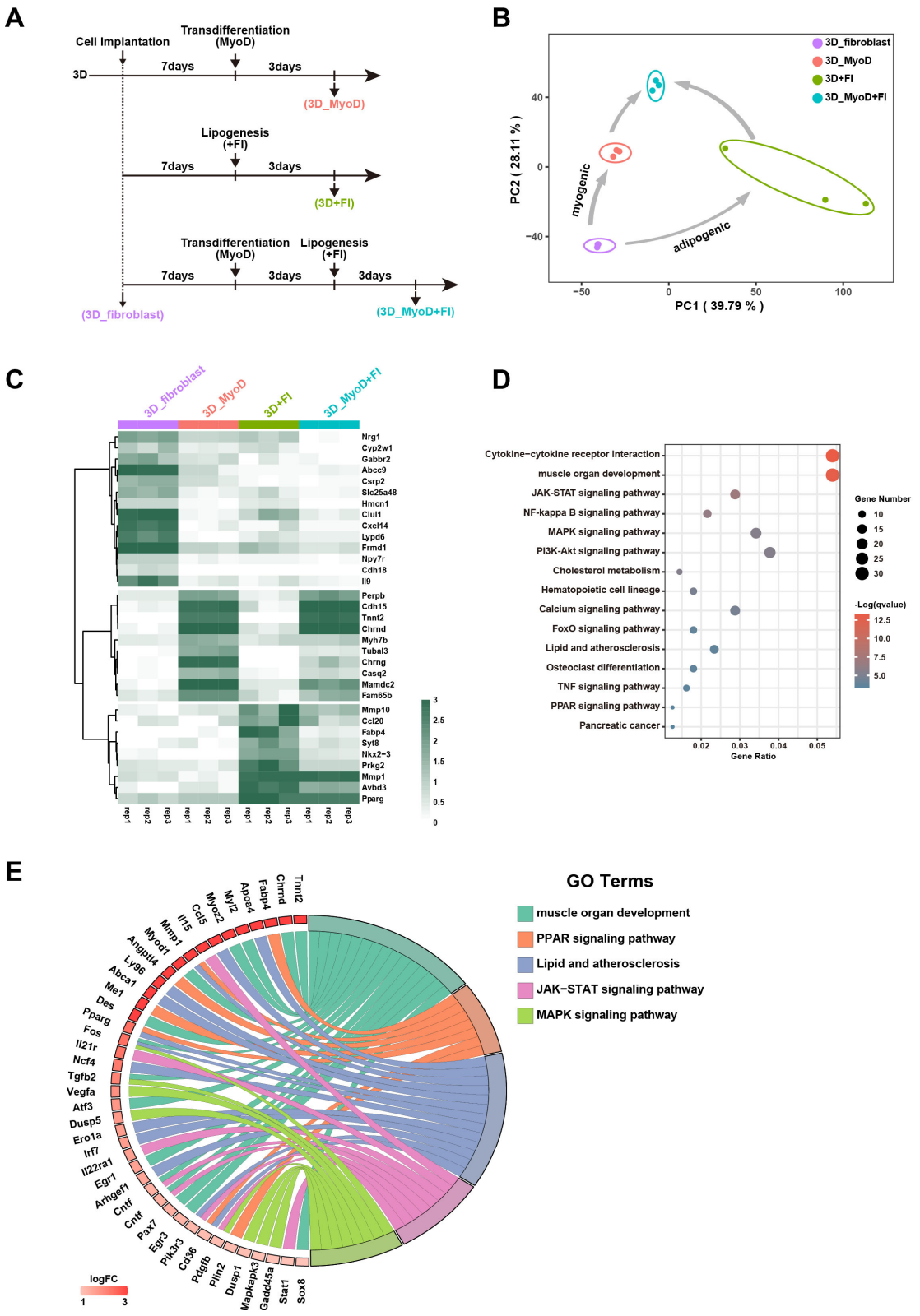

Figure 8. Gene expression profiles during transdifferentiation and fat deposition in 3D. (A) Scheme of the RNA-Seq samples marked by different color. (B) PCA analysis of transcriptome changes during myogenic transdifferentiation and fat deposition (n= 10,247 genes). The ellipses group include three biological replicates in each cell

type. The arrows represent the wiring of gene expression under different conditions. The routes were derived from original fibroblast toward two differentiation routes, namely “myogenic transdifferentiation” and “adipogenic transdifferentiation”. (C) Heat map showed the representative genes differentially expressed between 3D_MyoD+FI and 3D_fibroblast cells (n=3 biologically independent samples). (D) GO analysis of up-regulated DEGs between 3D_MyoD+FI vs. 3D_fibroblast cells. (E) GOChord analysis of the up-regulated genes within representative pathway between 3D_MyoD+FI and 3D_fibroblast cells.